



## CNS radiotherapy

# Clinical comparison of positional accuracy and stability between dedicated versus conventional masks for immobilization in cranial stereotactic radiotherapy using 6-degree-of-freedom image guidance system-integrated platform

Kazuhiro Ohtakara<sup>a,b,\*</sup>, Shinya Hayashi<sup>a,b</sup>, Hidekazu Tanaka<sup>b</sup>, Hiroaki Hoshi<sup>a</sup>, Masashi Kitahara<sup>b</sup>, Katsuya Matsuyama<sup>b</sup>, Hitoshi Okada<sup>b</sup>

<sup>a</sup> Department of Radiology, Gifu University Graduate School of Medicine; <sup>b</sup> Division of Radiation Oncology, Gifu University Hospital, Japan

## ARTICLE INFO

## Article history:

Received 1 June 2011

Received in revised form 17 October 2011

Accepted 20 October 2011

Available online 17 November 2011

## Keywords:

ExacTrac/Robotics

Frameless

Image-guided

Intrafractional movement

Novalis Tx

Stereotactic radiotherapy

## ABSTRACT

**Purpose:** To compare the positioning accuracy and stability of two distinct noninvasive immobilization devices, a dedicated (D-) and conventional (C-) mask, and to evaluate the applicability of a 6-degrees-of-freedom (6D) correction, especially to the C-mask, based on our initial experience with cranial stereotactic radiotherapy (SRT) using ExacTrac (ET)/Robotics integrated into the Novalis Tx platform.

**Materials and methods:** The D- and C-masks were the BrainLAB frameless mask system and a general thermoplastic mask used for conventional radiotherapy such as whole brain irradiation, respectively. A total of 148 fractions in 71 patients and 125 fractions in 20 patients were analyzed for the D- and C-masks, respectively. For the C-mask, 3D correction was applied to the initial 10 patients, and thereafter, 6D correction was adopted. The 6D residual errors (REs) in the initial setup, after correction (pre-treatment), and during post-treatment were measured and compared.

**Results:** The D-mask provided no significant benefit for initial setup. The post-treatment median 3D vector displacements (interquartile range) were 0.38 mm (0.22, 0.60) and 0.74 mm (0.49, 1.04) for the D- and C-masks, respectively ( $p < 0.001$ ). The post-treatment maximal translational REs were within 1 mm and 2 mm for the D- and C-masks, respectively, and notably within 1.5 mm for the C-mask with 6D correction. The pre-treatment 3D vector displacements were significantly correlated with those for post-treatment in both masks.

**Conclusions:** The D-mask confers positional stability acceptable for SRT. For the C-mask, 6D correction is also recommended, and an additional setup margin of 0.5 mm to that for the D-mask would be sufficient. The tolerance levels for the pre-treatment REs should similarly be set as small as possible for both systems.

© 2011 Elsevier Ireland Ltd. All rights reserved. Radiotherapy and Oncology 102 (2012) 198–205

The accuracy of patient immobilization and target alignment is a crucial prerequisite for cranial stereotactic radiosurgery (SRS) and has historically relied on a rigid invasive head frame that is currently still the *de facto* gold standard [1]. The use of an invasive frame, however, does not necessarily guarantee appropriate treatment accuracy, in as much as potential distortion or slippage of the frame could compromise treatment accuracy [1,2]. These undesirable events might be missed without an image-guidance system during treatment. Furthermore, the frame-based method has inherent shortcomings relating to patient comfort and safety, and clinical and technical workflow. Prior wide craniotomy could also render some patients ineligible for safe frame fixation.

Bolstered by a burgeoning interest in clinical applications, recent advances in image-guidance systems allowing for accurate and reproducible patient positioning have prompted us to perform frameless noninvasive SRS and fractionated stereotactic radiotherapy (SRT). In one such system Novalis Tx<sup>®</sup> (BrainLAB AG, Feldkirchen, Germany and Varian Medical Systems, Palo Alto, CA, USA), two potentially complementary forms of image-guidance system are supplied: ExacTrac (ET)/Robotics and On-Board Imager (OBI) [3,4]. The ET/Robotics system allows for 6-degrees-of-freedom (6D) setup verification and subsequent corrections to be made prior to or during treatment [5]. For cranial SRS/SRT, the ET/Robotics confers several advantages compared to the OBI: faster setup with IR-based guidance, faster acquisition of kV images, motion tracking in patients with IR reflectors directly attached to the mask, 6D verification and correction of the residual setup errors, and less radiation to the patient [3,4]. Recently, several studies have verified the accuracy of

\* Corresponding author. Address: Department of Radiology, Gifu University Graduate School of Medicine, 1-1 Yanagido, Gifu 501-1194, Japan.

E-mail address: [ohatakara@gifu-u.ac.jp](mailto:ohatakara@gifu-u.ac.jp) (K. Ohtakara).

the ET/Robotics system for the detection and correction of 6D quantitative offsets in both phantoms and patients, and the positional stability of the BrainLAB frameless radiosurgery mask system, which is comparable to that of the frame-based approach [1–3,6–8], although quality assurance germane to the geometric accuracy of the linkage among MV isocenter, treatment room lasers, and the ET system is indispensable at each institution to obviate potential systematic deviations [8–11].

At our institution, cranial SRS/SRT has been performed since 2005 using m3 micro-multileaf collimator (mMLC) (BrainLAB AG) as an add-on device to a non-dedicated linear accelerator, albeit without a dedicated image-guidance system. In December of 2009, Novalis Tx was installed, and the BrainLAB frameless mask system (hereafter referred to as a dedicated mask; D-mask) replaced an invasive frame for all cranial SRS/SRT cases except for patients harboring arteriovenous malformations. After one month of experience with a few cases to adapt ourselves to the treatment system, we prospectively evaluated the pre- and post-treatment 6D residual errors (REs) with the ET to assess the positional accuracy and stability for each patient and to use the results as a reference in patient follow-up. The D-mask has been the principal immobilization device for cranial SRS/SRT at our institution, while the mask used for conventional radiotherapy (cRT), such as whole brain irradiation (hereafter referred to as a conventional mask, or C-mask), was applied to some patients with the expectation of achieving positional stability of <3 mm. These patients received a low-dose SRT boost following cRT or were deemed ineligible for tight immobilization with the D-mask for various reasons: cervical pain/discomfort resulting from severe kyphosis or spinal metastases, or occipital pain attributable to titanium plates used for prior craniotomy [12]. Given the differences in the physical properties of the two masks, the positional stability of the C-mask is assumed to be less than that of the D-mask, and one, therefore, may hesitate to apply 6D correction to the C-mask, which is worrisome because of secondary patient movements that might jeopardize the patients [13]. To date, the differences in positional accuracy and stability between these two masks and the applicability of 6D correction to the C-mask have yet to be fully examined, although the differences among several immobilization methods by using general masks with cone-beam computed tomography (CT)-based image guidance have been recently investigated [14].

In this study, we compared the positional accuracy and stability of D- versus C-masks and evaluated the applicability of 6D correction, especially to the C-mask, based on our initial year of experience with cranial SRS/SRT with ET/Robotics-based image guidance on the Novalis Tx platform.

## Materials and methods

### Study populations and evaluation methods with ExacTrac/Robotics

From January to December 2010, a total of 148 fractions in 71 patients and 125 fractions in 20 patients were evaluable for the D- and C-mask, respectively. Demographic data for the patients and treatment characteristics are summarized in [Supplementary Table 1](#). These include head and neck lesions amenable to the skull-anatomy alignment with the ET. For purposes of planning, CT images were acquired for each patient with LightSpeed Xtra (General Electric Medical Systems, Waukesha, WI, USA) with a slice thickness of 1.25 mm. The dynamic conformal arc (DCA) technique was used in all treatment planning, and the plans were generated, using both iPlan Image ver 4.1 and iPlan Dose ver 4.1 treatment planning system (TPS). Patients were immobilized with either the D-mask fixed to the couch extension or the C-mask (E-frame, ES-01, Engineering System Co., Ltd., Matsumoto, Japan) placed on the couch ([Supplementary Fig. 1a,b](#)).

The ET/Robotics system mainly consists of an infrared (IR)-based optical tracking system for initial patient positioning and guidance for the adjustment of couch movement, and a dual stereoscopic kV X-ray imaging system for position verification based on internal bony anatomy, and ExacTrac 5.5.2 fusion software. The details of the ET/Robotics system and the image-guidance procedures were already described elsewhere [1–11]. After mask application and patient pre-positioning with the IR-based guidance system, the X-ray images were obtained with settings of 100 kV, 100 mA, and 100 ms. To determine the 6D REs, the images were matched with digitally reconstructed radiographs (DRRs) generated from the planning CT images, and the 6D offsets were computed. The accuracy of fusion is influenced by imaging parameters and variations in anatomy and, therefore, must be carefully reviewed [1]. Determination of a fusion region of interest (ROI) by masking for the exclusion of potentially deviated structures, e.g., the mandible, upper cervical spine, or IR reflectors, relative to the skull, and verification of the fusion results were performed by the first author in all cases except for a few cases in second or later fractions in SRT.

The 6D REs at initial setup were a measure of the repositioning accuracy of both masks without the use of the X-ray imaging. If a translational RE > 2.5 mm or rotational error > 2.5° (later > 2.0°) was detected at the initial setup, the mask was re-applied to avoid large-scale corrections (>2.5 mm or >2°). For this purpose, radiation therapists were familiarized in advance with the coordinate system defined in the ET system ([Supplementary Fig. 2](#)). Subsequently, 6D or 3D couch correction was executed automatically by Robotics, and the second X-ray verification was performed. For some time from the beginning of image-guided cranial SRT, the tolerance levels for pre-treatment REs were different between the masks: <0.5 mm/° for the D-mask, <1.0 mm/° for the C-mask. If a one-time correction did not satisfy these ranges, additional correction was done. After treatment, the X-ray images were acquired. The difference between the post- and pre-treatment REs was used as a surrogate measure of intrafractional patient movement. When treating multiple lesions, data for REs at initial patient setup and after correction by Robotics were collected for the first lesion, and those for intrafractional movements (IMs) were obtained from the last one. A total of 131 fractions for the D-mask and all 125 fractions for the C-mask were evaluable for IMs.

Each 6D RE, i.e. three translations in lateral (Lat), longitudinal (Long), and vertical (Vert) directions and three rotations around each axis (pitch, roll, and yaw, respectively) was uniformly described as the deviation from zero with reference to the coordinate system ([Supplementary Fig. 2](#)). The 3D vector displacements were calculated as root sum of squares from the three translational REs.

### Quality assurance for cranial SRS/SRT at our institution

The geometric linkage among the megavoltage isocenter, room laser, and the ET system was checked each day before treatment. The Winston–Lutz test was used to verify the linkage between MV isocenter and the isocenter defined by treatment room lasers as described elsewhere [8–10]. The alignment of the ET system to the room lasers was verified using a  $10 \times 10$  cm<sup>2</sup> flat isocenter phantom with five IR-reflective markers [8,9]. The tolerance level for the deviation was <0.3 mm in either of the three translational directions. If a deviation >0.3 mm in any direction or a deviation >0.25 mm that was repeated a few times was detected, calibration of the system was performed as described.

### Attempts at improving positional accuracy and stability at our institution

Before treatment, patients were given detailed explanations of the treatment workflow, especially the 6D couch correction and

subsequent couch rotations for non-coplanar arcs. We also requested each patient to let us know immediately whenever they moved involuntarily due to, e.g., a fit of coughing or if continued treatment became unbearable. During treatment, radiation therapists always let the patients know of the adjustable couch movements before operations, to circumvent possible patient motions caused by a surprise reaction to an abrupt couch adjustment. For patients with dentures, those were not removed at treatment.

For D-mask fabrication, the positions and configurations of the caudal edge of each earlobe were marked with an oil-based felt-tip pen as a guide for the *Long* direction to expedite the initial positioning (Supplementary Fig. 1c). The C-mask was applied to each patient with greater attention than the cRT and fixed to the top of the extended couch with tape during treatment (Supplementary Fig. 1b).

With regard to treatment planning, we adopted simplified arc arrangements as reasonably as possible such that 3–5 arcs containing 1–2 coplanar arcs were mainly used, with the expectation that shorter treatment time can lighten the patient's burden and might lead to smaller IMs. Plans were mainly optimized by leaf margin adjustment in increments of 0.1 mm, couch/collimator angle optimization, or beam shaping techniques with manual fine adjustment of the selected leaves [15]. All treatments were done in the 6 MV X-ray energy mode at a dose rate of up to 1000 MU/min. The typical time period between acquisition of the first X-ray image and completion of irradiation for each target was 12–15 min.

### Statistical analyses

Statistical analyses were performed using PASW Statistics 18.0 (SPSS Inc., Chicago, IL Illinois, USA). The Shapiro–Wilk test was used to test the normality of the data distribution. In fact, the hypothesis of a normal distribution was rejected with the Shapiro–Wilk test for a considerable number of variables (Figs. 1 and 2, Supplementary Fig. 3 and Supplementary Table 2). Therefore, we basically chose non-parametric tests for the following analyses. Box-and-whisker plots (BWPs) were used to represent the distribution of variables. In the BWP, the whiskers denote the nearest values <1.5 times the interquartile range (IQR). The open circles beyond the lines indicate the individual outliers <3.0 times the IQR. The stars beyond the lines indicate extreme values ( $\geq 3.0$  times the IQR).

Comparison of two variables was performed using Fisher's exact test for categorical variables, the Mann–Whitney *U* test for numerical variables, and Levene's test for equality of variances in numerical variables. Spearman's rank correlation coefficient was applied to evaluate any correlations between the variables. Linear curve-fitting with the correlation coefficient determinant  $R^2$  was also implemented. All *p*-values were calculated with two-tailed tests, and the criterion for statistical significance was considered to be  $p < 0.05$ .

## Results

### REs at initial positioning

The 6D REs at initial patient setup before re-application of the mask, if performed, are shown in Fig. 1a. The median *Long* value significantly departed from zero for the D-mask. The 3D vector displacements for the C-mask were smaller than those for the D-mask ( $p = 0.002$ ), albeit with a difference in the median value of 0.2 mm (Supplementary Table 2a). None of the differences in variance of the REs were statistically significant between the two masks.

### REs at pre-treatment (post-correction)

The translational REs were almost entirely within the range of  $\pm 0.5$  mm for both masks (Fig. 1b). The rotational REs for the

D-mask were generally within  $\pm 0.5^\circ$ , whereas those for the C-mask were significantly larger. The variances in the *Long* and three rotations were significantly larger for the C-mask. No significant differences were observed in the 3D vector.

### Post-treatment REs and intrafractional movements

After treatment, the 6D REs for the D-mask were within  $\pm 1.0$  mm/ $^\circ$ , except for a few outliers in the *Yaw* (Fig. 1c). On the contrary, the translational and rotational REs for the C-mask were generally within  $\pm 1.5$  mm and  $\pm 2.0^\circ$ , respectively, although the *Long* and *Roll* values were slightly beyond 1.5 mm and  $-2.0^\circ$ , respectively. All the variances for the 6D REs were significantly smaller for the D-mask. The 3D vector displacements were also significantly smaller with the D-mask (Supplementary Table 2a and Supplementary Fig. 4).

All variables for the IMs departed from normal distributions (Fig. 1d). The variances for the 6D IMs were significantly greater for the C-mask, except for the *Yaw*. The equivalent or smaller post-treatment 3D vector displacements compared to those for pre-treatment can be regarded as permissible or preferable IMs, and these cases were observed in 34 of 131 fractions (26.0%) and 6 of 125 fractions (4.8%) for the D- and C-masks, respectively ( $p < 0.001$ , by Fisher's exact test). Among them, however, differences of  $>0.2$  mm were noted in 4 and 1 fraction(s) of the D- and C-masks, respectively ( $p = 0.371$ ). Table 1 compares the IMs that we obtained with those obtained by other institutions, where data were alternatively expressed as mean value ( $\pm 1$  standard deviation, SD) for consistency [16].

The pre-treatment 3D vector displacements were significantly correlated with those for post-treatment for both masks (Fig. 3).

### Comparison of 3D versus 6D correction for C-mask

A total of 73 and 52 fractions were compared for 3D versus 6D corrections, respectively. Before treatment, no significant differences in the translational REs were observed between two groups, whereas the rotational REs were significantly smaller for the 6D group, except for the median *Roll* value (Fig. 2a). The rotational REs for the 6D group were within  $\pm 1.0^\circ$ , except for two outliers.

After treatment, the 6D REs for the 6D group were within  $\pm 1.5$  mm/ $^\circ$ , except for two outliers in the rotation variables (Fig. 2b). The variances for the 6D REs except for the *Lat* were significantly smaller for the 6D group. No significant differences in the pre- and post-treatment 3D vector displacements were observed between two groups (Supplementary Table 2b).

For the IMs, none of the variances for the 6D REs were significantly different between two groups (Supplementary Fig. 3). The 6D IMs were within  $\pm 1.5$  mm/ $^\circ$  for both groups, except for three outliers in the *Long* for the 3D group.

## Discussion

The thrust of the present study is also regarded as an attempt to examine whether the D-mask provides the positional accuracy and stability comparable to the data reported by other institutions and how the C-mask compares to the D-mask as a benchmark.

In other studies, the RE variables have been generally represented as mean (systematic error)  $\pm 1$  SD and/or root-mean-square (random error), based on the assumption that the variables are normally distributed [17]. A considerable number of the variables in this study, however, substantially departed from a normal distribution. Given that most of these variables departing from normal distributions showed low skewness values (data not shown), SDs are not necessarily suitable for the representation of random errors.

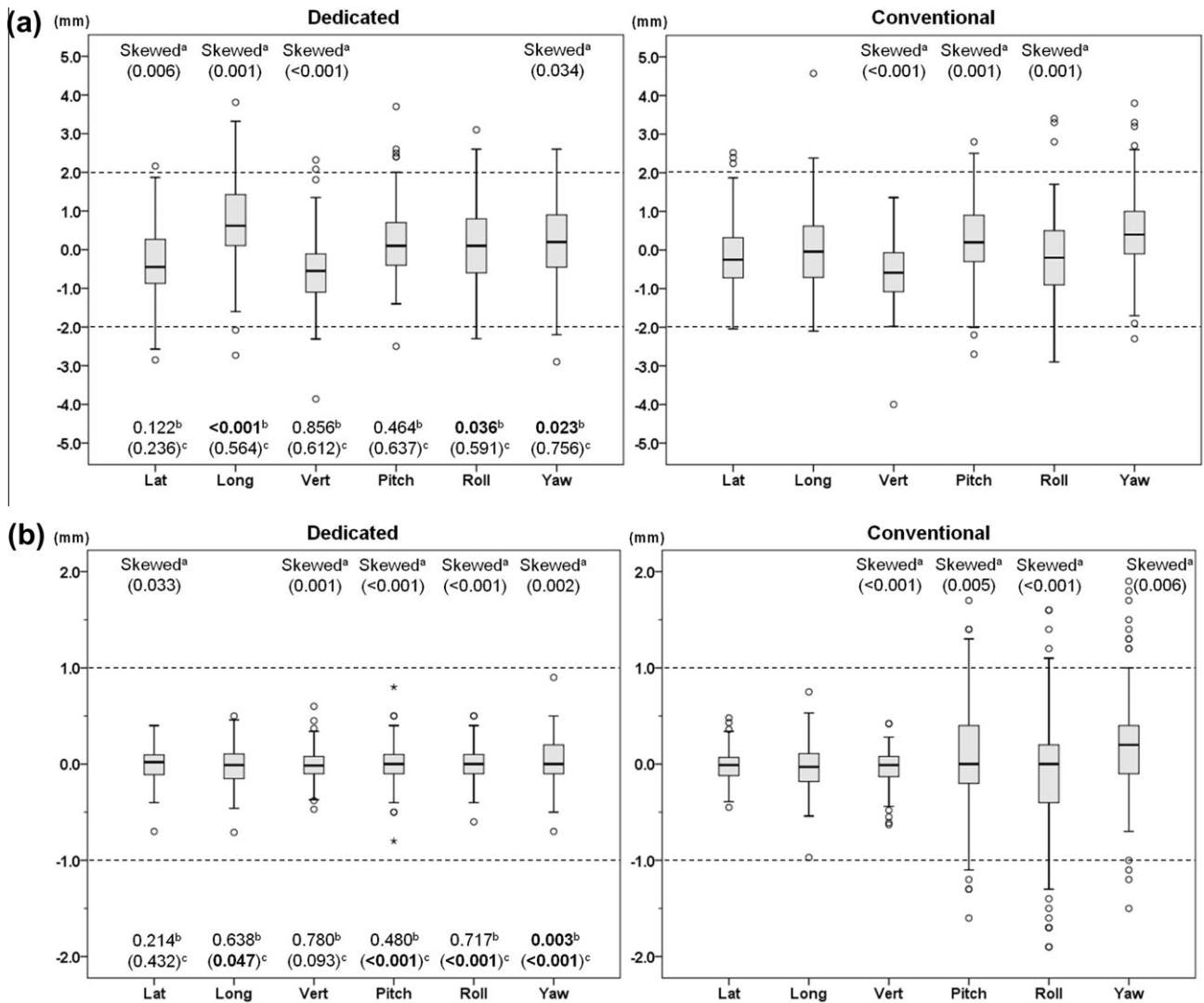


**Fig. 1.** Comparison of D- and C-masks with respect to 6D residual errors at initial setup (a), after correction (pre-treatment) (b), post-treatment (c), and for intrafractional movements (d). <sup>a</sup>Variables departing from a normal distribution based on Shapiro–Wilk test (*p* values in parenthesis). <sup>b</sup>*p* values by Mann–Whitney *U*-test. <sup>c</sup>*p* values by Levene's test. Significant results are shown in boldface.

For data in such variables, the BWP would be a suitable method to represent the data distribution rather than the former method.

#### Differences in positional accuracy and stability between the two masks

Unexpectedly, the D-mask provided no significant advantage for initial positioning compared to the C-mask. The C-mask generally showed smaller 6D REs than we assumed. The upper jaw support that came with the earlier model was unavailable in the current D-mask used in this study [6], and we, therefore, marked the earlobe positions on the D-mask as a guide. Nevertheless, a significant shift in the *Long* variable to the cranial direction was observed for the D-mask. The positioning of the pillow (head support) in the C-mask is adjustable according to the patient's head position, whereas the posterior part of the D-mask was fixed to the treatment couch, accordingly requiring direct adjustment of the patient's position. These differences may be attributable to the larger *Long* REs for the D-mask. At the least, inasmuch as a number of the REs >2 mm/° were observed for both masks, in each case image-guidance with 6D verification and correction is equally essential for either immobilization system.

After 6D or 3D correction, the 6D REs for both masks were significantly reduced except for three rotational REs in the C-mask

with 3D correction. In a few cases, however, translational REs >0.5 mm were still observed. These REs may either result from inadequate correction by the Robotics or secondary patient movements induced by couch correction. In fact, we permitted these REs without further correction to save time in cases with planned multi-target treatment, or in consideration of the patient's comfort. As stated previously, the tolerance levels with respect to the pre-treatment 6D REs were different between the masks. However, the pre-treatment 3D vector displacements were significantly correlated with those for post-treatment (Fig. 3), and preferable IMs were rare. These results imply that the tolerance levels for pre-treatment REs should be set as small as possible in either mask system to minimize the post-treatment REs. The Robotics, however, does not necessarily correct the 6D REs automatically to the level of <0.3 mm/° with one-time operation. Inasmuch as the 6D or 3D couch correction is executed with the IR-based guidance system in increments of 0.5 mm/° (minimum adjustable ranges), the Robotics may not further correct a RE of <0.5 mm/° (e.g. 0.45 mm), in which case manual fine correction of the specific RE may be necessary to attain a further more precise adjustment.

The IMs for the D-mask were generally comparable to those reported by other institutions (Table 1). Our results also endorse the previous studies concluding that frameless radiosurgery permits



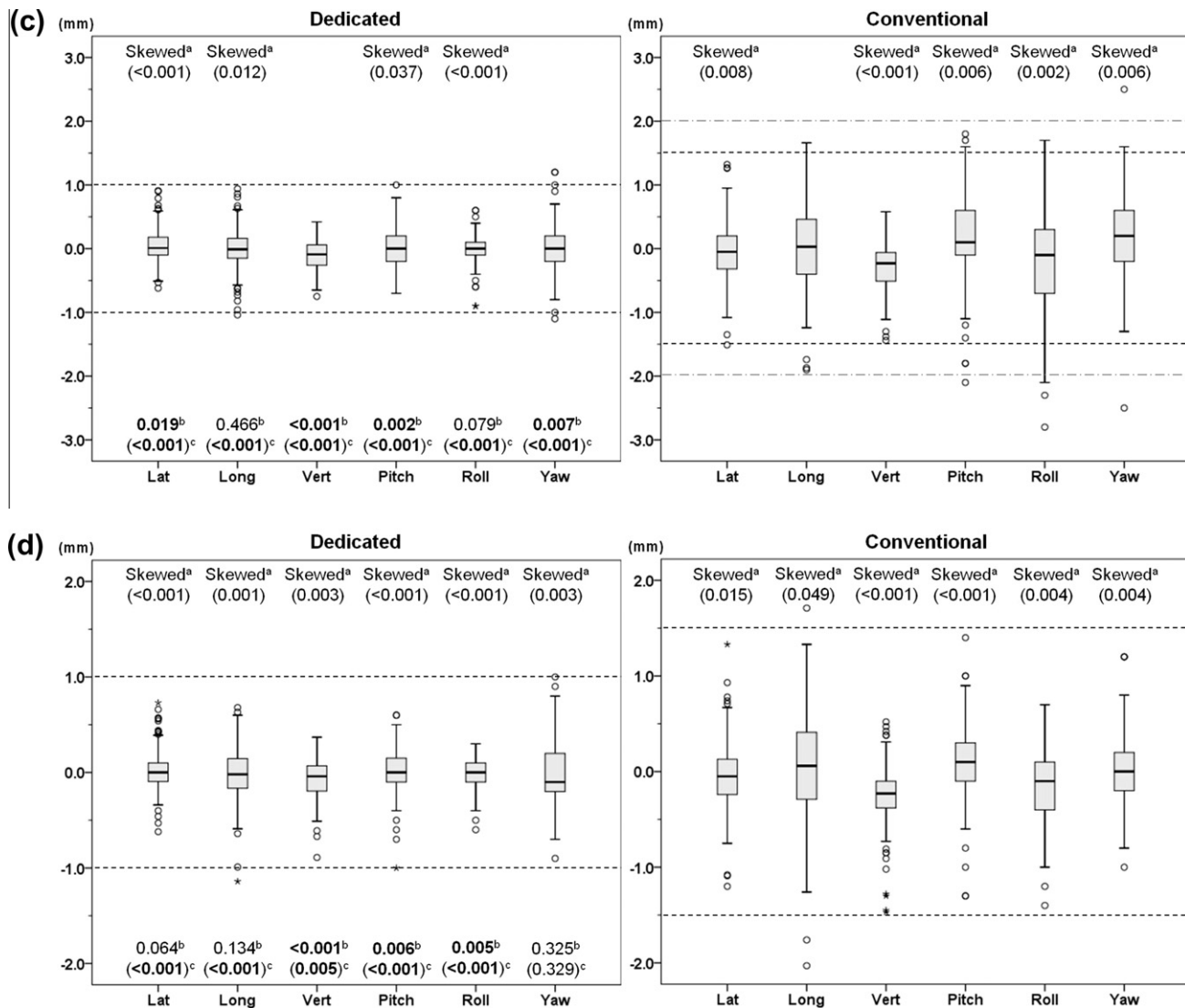


Fig. 1 (continued)

comparable positional accuracy to the frame-based approach. On the other hand, the IMs for the C-mask were generally smaller than those with immobilization by using similar general masks reported by Tryggstad et al. [14] or Linthout et al. [16] to which our several attempts to improve the treatment accuracy might contribute. Ramakrishna et al. reported that the *Long* REs for the BrainLAB mask system were significantly larger than those of the frame-based approach [1]. In our data, on the contrary, the *Long* REs for the D-mask were smaller and even comparable to those of the BRW frame.

Given the physical properties of the C-mask in comparison of those for the D-mask, we had misgivings about possible secondary patient movements inside the mask induced by 6D couch correction and, therefore, initially applied 3D correction to the C-mask. Later, we also prudently applied 6D correction to the C-mask within the ranges of <2.5 mm and <2.0° (rarely <2.5°), considering the unexpectedly smaller IMs. The pre-treatment rotational REs for the C-mask were significantly improved by 6D correction compared to those with 3D correction. Given the non-significant differences in the pre-treatment translational REs between 3D and 6D correction and the post-treatment translational REs to within 1.5 mm for the C-mask with 6D correction, the results imply that the 6D correction within the above ranges induces no significant adverse events and rather confers a more accurate 6D setup. Therefore, 6D correction is also recommended for the C-mask.

The D-mask certainly provided superior positioning stability than the C-mask and is a preferable immobilization device for cranial SRS/SRT, especially for lesions located in or juxtaposed next to a critical structure. There are, however, some patients deemed unsuitable for the D-mask use as mentioned previously [12]. Meanwhile, the C-mask has several merits: more porous structure leading to less discomfort and flexibility in the height of a pillow for initial positioning of the head. When used as a boost following cRT, the patients may adapt themselves sufficiently to the mask. The IQR of the post-treatment 3D vector displacements was almost within 1.0 mm for the C-mask in its entirety (Supplementary Table 2). In the study populations, 6D correction was still applied to only a modest number of patients with the C-mask, which hindered a firm conclusion. Overall treatment accuracy using the C-mask may be improved by further familiarization with this system. At the least, it seems valuable to have an alternative to the D-mask. High precision treatment with the C-mask would be also useful in patients who receive a large number of SRT fractions for indications such as optic nerve sheath meningioma. Given the physical properties, the observed IMs for the C-mask can be taken as an upper limit for non-invasive immobilization devices. Superior positional stability would be expected when the used mask is utilized with a reinforcing band.

To determine the optimal setup margin for frameless SRS/SRT, the comprehensive uncertainty analyses of the treatment system

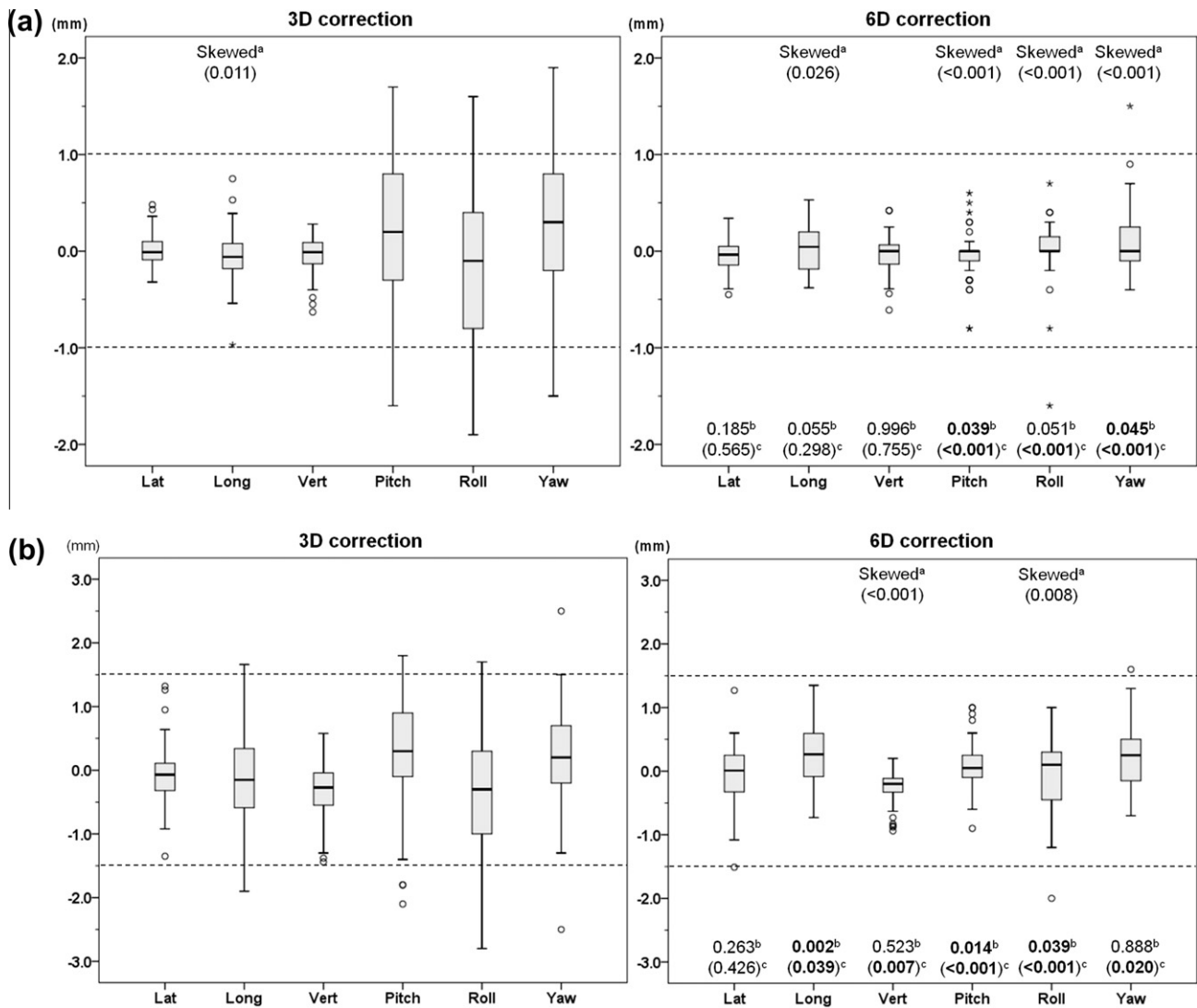


Fig. 2. Comparison of 6D residual errors in C-mask 3D and 6D corrections with respect to pre-treatment (a) and post-treatment (b).

Table 1

Comparison of intrafractional movements.

Author, year, [ref]	Immobilization	Pt (Fr)	Lat	Long	Vert	3D Vector	Pitch	Roll	Yaw
van Santvoort et al. (2008) [6]	Dedicated (UJS)	20 (192)	-0.11 (0.20)	0.05 (0.28)	0.01 (0.10)	0.59 (0.17)	0.02 (0.23)	-0.05 (0.31)	0.02 (0.22)
	Dedicated (VMP)	20 (203)	-0.11 (0.16)	0.13 (0.13)	-0.03 (0.06)	0.44 (0.13)	-0.02 (0.15)	-0.02 (0.11)	0.06 (0.17)
Lamba et al. (2009) [2]	Dedicated	79 (214)	0.0 (0.3)	-0.1 (0.5)	0.1 (0.3)	NA	NA	NA	NA
Verbakel et al. (2010) [8]	Dedicated	46 (135)	-0.04 (0.23)	0.01 (0.38)	-0.06 (0.19)	NA	0.00 (0.20)	-0.03 (0.15)	0.07 (0.34)
Present study	Dedicated	63 (131)	0.02 (0.23)	-0.02 (0.28)	-0.07 (0.21)	0.17 (0.24)	-0.02 (0.29)	-0.02 (0.33)	0.01 (0.25)
	Conventional	20 (125)	-0.01 (0.40)	0.16 (0.46)	-0.26 (0.34)	0.42 (0.37)	-0.11 (0.39)	0.12 (0.28)	0.14 (0.39)
Linthout et al. (2006) [16]	Conventional	13 (385)	0.00 (0.7)	0.30 (0.7)	-0.5 (1.2)	NA	-0.2 (0.8)	0.1 (0.7)	-0.1 (0.6)
Tryggstad et al. (2011) [14]	Device 1 <sup>a</sup>	7 (59)	0.06 (0.7)	0.02 (0.6)	-0.12 (0.8)	NA	-0.17 (0.9)	0.09 (0.6)	0.05 (0.8)
	Device 2 <sup>b</sup>	9 (67)	0.26 (0.7)	0.10 (0.7)	-0.26 (0.5)	NA	0.12 (0.6)	0.10 (0.5)	-0.05 (0.8)
	Device 3 <sup>c</sup>	16 (102)	0.06 (0.5)	-0.23 (0.6)	0.04 (0.4)	NA	0.06 (0.6)	0.04 (0.5)	0.20 (0.6)
	Device 4 <sup>d</sup>	8 (44)	0.03 (0.3)	-0.29 (0.6)	-0.14 (0.4)	NA	-0.06 (0.4)	-0.17 (0.5)	-0.06 (0.6)

Abbreviations: Pt (Fr), Patient (Fractions); UJS, upper jaw support; VMP, vacuum mouth piece; NA, not available.

<sup>a</sup> Type-S intensity-modulated radiotherapy (head only) mask (Civco, Kalona, IA, USA) with head cushion.

<sup>b</sup> Uni-Frame mask (Civco) with head cushion, coupled with a BlueBag body immobilizer (Medical Intelligence, Schwabmünchen, Germany).

<sup>c</sup> Type-S head and shoulder mask with head and shoulder cushion (Civco).

<sup>d</sup> Same as Device C, coupled with a mouthpiece.

are indispensable [9,10], in addition to the uncertainty for target localization such as the accuracy of CT-MRI fusion. These parameters include the shift in position among the MV isocenter, center of room lasers and central point detected with the ExacTrac system, the uncertainty of the MV isocenter position with gantry and couch rotation, the uncertainty of the ExacTrac software for verification of

image fusion, the positional reproducibility and accuracy of the ExacTrac Robotics, and intra-fractional patient motion (the accuracy of patient immobilization). Therefore, we cannot refer to the optimal setup margins for each mask from the results of our study and should focus on the differences in positional stability between two masks. The posttreatment 3D vector displacements values <1.5

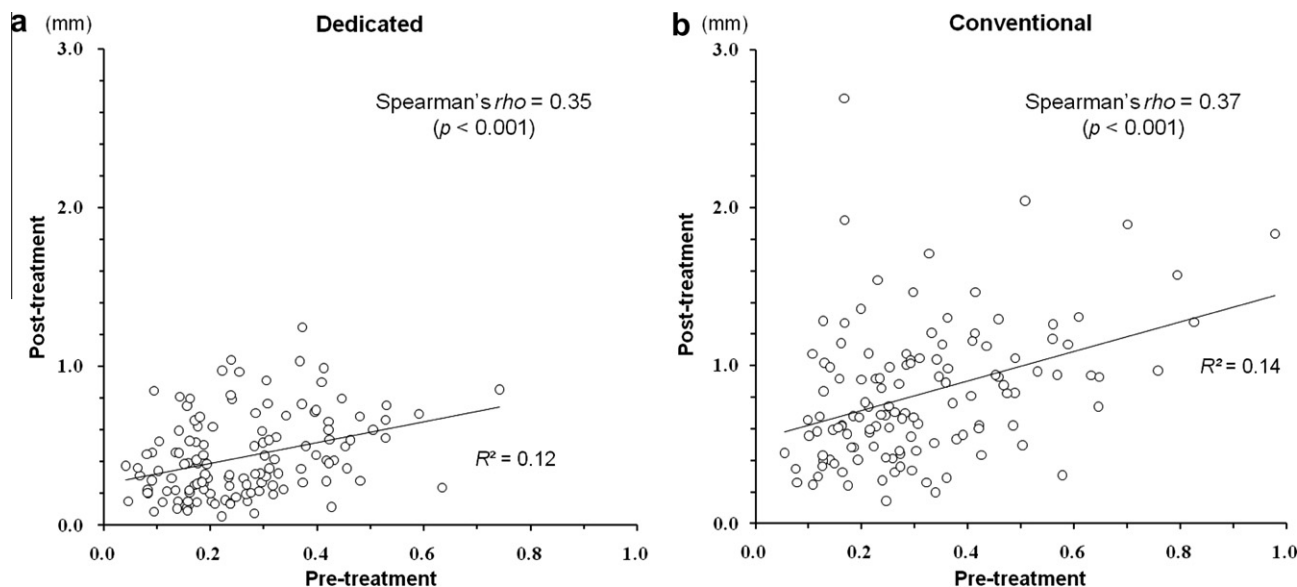


**Fig. 3.** Correlation between pre- and post-treatment translational residual errors in 3D vector displacements. (a) D-mask. (b) C-mask.

times IQR for the C-mask were within 1.5 mm irrespective of correction methods, and the differences between the C- and D-masks were within 0.5 mm (Supplementary Fig. 4). Based on these findings, an additional isotropic margin of 0.5 mm to that for the D-mask would be sufficient for the C-mask with 6D correction. Meanwhile, presence of the outliers cannot be ignored, and, therefore, it is recommended to verify routinely the post-treatment 6D REs for each patient to determine whether the treatment was executed with the expected positional stability.

#### Study limitations

There exist several limitations in this study, especially relating to our initial experience with the ET/Robotics system. There was no denying that obvious selection bias existed in the allocation of each mask system and that the presented results could have been influenced by the level of experience of the first author learning to determine the fusion ROI.

The differences between the pre- and post-treatment REs were used as a measure of IM. Although no significant IMs were observed based on the real-time IR-based tracking for the C-mask, this method cannot directly track the patient's position inside the mask. Consequently, we may miss potentially significant patient movement in the midst of treatment.

The consistency of the spatial relationship between the target and skull is an undisputed prerequisite for image-guidance based on bony anatomy alignment. In clinical practice, however, target deviation inside the skull attributable to alleviation of perilesional edema by concomitant anti-edema treatment or geometrical change of the target owing to early tumor shrinkage may occur during or even prior to treatment [18]. Image-guidance by bony anatomy alignment does not necessarily guarantee true target alignment for every SRT fraction, especially for longer treatment periods of more than one week. Precautions, therefore, need to be taken against these possibilities with careful neurological monitoring or neuroimaging evaluation if needed.

#### Conclusions

We evaluated our initial year of experience with frameless image-guided cranial SRS/SRT by using the ET/Robotics integrated in

the Novalis Tx platform. The D-mask confers positional stability acceptable for the implementation of SRS/SRT. For the C-mask, 6D correction can be safely executed and is also recommended for accurate positioning. Although the IMs for the C-mask were certainly larger than those for the D-mask, an additional setup margin of 0.5 mm to that for the D-mask would be sufficient for the C-mask with 6D correction. The tolerance levels for pre-treatment REs should similarly be set as small as possible for both masks to minimize the post-treatment REs. Further clinical investigations are needed to validate the adequacy of these findings and to determine whether frameless radiosurgery is a legitimate alternative to frame-based SRS for various indications.

#### Conflict of interest statement

The authors of this study have nothing to disclose.

#### Appendix A. Supplementary data

Supplementary data associated with this article can be found, in the online version, at [doi:10.1016/j.radonc.2011.10.012](https://doi.org/10.1016/j.radonc.2011.10.012).

#### References

- [1] Ramakrishna N, Rosca F, Friesen S, Tezcanli E, Zygmanski P, Hacker F. A clinical comparison of patient setup and intra-fraction motion using frame-based radiosurgery versus a frameless image-guided radiosurgery system for intracranial lesions. *Radiother Oncol* 2010;95:109–15.
- [2] Lamba M, Breneman JC, Warnick RE. Evaluation of image-guided positioning for frameless intracranial radiosurgery. *Int J Radiat Oncol Biol Phys* 2009;74:913–9.
- [3] Ma J, Chang Z, Wang Z, Jackie Wu Q, Kirkpatrick JP, Yin FF. ExacTrac X-ray 6 degree-of-freedom image-guidance for intracranial non-invasive stereotactic radiotherapy: comparison with kilo-voltage cone-beam CT. *Radiother Oncol* 2009;93:602–8.
- [4] Kim J, Jin JY, Walls N, et al. Image-guided localization accuracy of stereoscopic planar and volumetric imaging methods for stereotactic radiation surgery and stereotactic body radiation therapy: a phantom study. *Int J Radiat Oncol Biol Phys* 2011;79:1588–96.
- [5] Jin JY, Yin FF, Tenn SE, Medin PM, Solberg TD. Use of the BrainLAB ExacTrac X-Ray 6D system in image-guided radiotherapy. *Med Dosim* 2008;33:124–34.
- [6] van Santvoort J, Wiggensraad R, Bos P. Positioning accuracy in stereotactic radiotherapy using a mask system with added vacuum mouth piece and stereoscopic X-ray positioning. *Int J Radiat Oncol Biol Phys* 2008;72:261–7.

- [7] Feygelman V, Walker L, Chinnaiyan P, Forster K. Simulation of intrafraction motion and overall geometrical accuracy of a frameless intracranial radiosurgery process. *J Appl Clin Med Phys* 2008;9:2828.
- [8] Verbakel WF, Lagerwaard FJ, Verduin AJ, Heukelom S, Slotman BJ, Cuijpers JP. The accuracy of frameless stereotactic intracranial radiosurgery. *Radiother Oncol* 2010;97:390–4.
- [9] Hayashi N, Obata Y, Uchiyama Y, Mori Y, Hashizume C, Kobayashi T. Assessment of spatial uncertainties in the radiotherapy process with the Novalis system. *Int J Radiat Oncol Biol Phys* 2009;75:549–57.
- [10] Takakura T, Mizowaki T, Nakata M, et al. The geometric accuracy of frameless stereotactic radiosurgery using a 6D robotic couch system. *Phys Med Biol* 2010;55:1–10.
- [11] Gevaert T, Verellen D, Tournel K, et al. Setup Accuracy of the Novalis ExacTrac 6DOF System for Frameless Radiosurgery. *Int J Radiat Oncol Biol Phys* 2011; [doi:10.1016/j.ijrobp.2011.01.052](https://doi.org/10.1016/j.ijrobp.2011.01.052).
- [12] Bednarz G, Machtay M, Werner-Wasik M, et al. Report on a randomized trial comparing two forms of immobilization of the head for fractionated stereotactic radiotherapy. *Med Phys* 2009;36:12–7.
- [13] Linthout N, Verellen D, Tournel K, Reynders T, Duchateau M, Storme G. Assessment of secondary patient motion induced by automated couch movement during on-line 6 dimensional repositioning in prostate cancer treatment. *Radiother Oncol* 2007;83:168–74.
- [14] Tryggestad E, Christian M, Ford E, et al. Inter- and Intrafraction Patient Positioning Uncertainties for Intracranial Radiotherapy: A Study of Four Frameless, Thermoplastic Mask-Based Immobilization Strategies Using Daily Cone-Beam CT. *Int J Radiat Oncol Biol Phys* 2011;80:281–90.
- [15] Leavitt DD. Beam shaping for SRT/SRS. *Med Dosim* 1998;23:229–36.
- [16] Linthout N, Verellen D, Tournel K, Storme G. Six dimensional analysis with daily stereoscopic x-ray imaging of intrafraction patient motion in head and neck treatments using five points fixation masks. *Med Phys* 2006;33: 504–13.
- [17] van Herk M. Errors and margins in radiotherapy. *Semin Radiat Oncol* 2004;14:52–64.
- [18] Guckenberger M, Baier K, Guenther I, et al. Reliability of the bony anatomy in image-guided stereotactic radiotherapy of brain metastases. *Int J Radiat Oncol Biol Phys* 2007;69:294–301.